Mathematical Biosciences and Engineering

MBE, 21 (3): 4328–4350.
DOI: 10.3934/mbe.2024191
Received: 09 January 2024
Revised: 06 February 2024
Accepted: 13 February 2024
Published: 26 February 2024

https://www.aimspress.com/journal/MBE

Research article

Advancing glioma diagnosis: Integrating custom U-Net and VGG-16 for improved grading in MR imaging

Sonam Saluja [1,*], Munesh Chandra Trivedi [1], and Shiv S. Sarangdevot [2]

[1] Department of Computer Science and Engineering, National Institute of Technology Agartala, Tripura,799046, India
[2] Janardan Rai Nagar Rajasthan Vidyapeeth, Udaipur 313001, India

* **Correspondence:** Email: sonamcse.sch@nita.ac.in.

Abstract: In the realm of medical imaging, the precise segmentation and classification of gliomas represent fundamental challenges with profound clinical implications. Leveraging the BraTS 2018 dataset as a standard benchmark, this study delves into the potential of advanced deep learning models for addressing these challenges. We propose a novel approach that integrates a customized U-Net for segmentation and VGG-16 for classification. The U-Net, with its tailored encoder-decoder pathways, accurately identifies glioma regions, thus improving tumor localization. The fine-tuned VGG-16, featuring a customized output layer, precisely differentiates between low-grade and high-grade gliomas. To ensure consistency in data pre-processing, a standardized methodology involving gamma correction, data augmentation, and normalization is introduced. This novel integration surpasses existing methods, offering significantly improved glioma diagnosis, validated by high segmentation dice scores (WT: 0.96, TC: 0.92, ET: 0.89), and a remarkable overall classification accuracy of 97.89%. The experimental findings underscore the potential of integrating deep learning-based methodologies for tumor segmentation and classification in enhancing glioma diagnosis and formulating subsequent treatment strategies.

Keywords: gliomas; deep learning; segmentation; classification; U-Net; VGG-16

1. Introduction

The human brain, the most intricate organ in the human body, orchestrates an array of vital

biological functions, including respiration and muscular control. However, when a mass of cells undergoes abnormal growth within or adjacent to the brain, it culminates in a formidable challenge—brain tumors. Among these, gliomas [1] emerge as one of the most common categories of glial-based primary tumors in adults. They exhibit varying degrees of malignancy, encompassing Grade I to Grade IV, as classified by World Health Organization [2,3]. Grades I and II are typically deemed benign or low-grade (LGG), while Grades III and IV are classified as malignant or high-grade (HGG) [4]. Grade I tumors grow slowly and are sometimes entirely resectable with surgery, but Grade IV tumors are aggressive, rapidly growing, and challenging to treat. The most frequent primary tumors were astrocytomas (38.7%), with HGGs (59.5%) making up the majority [4]. Despite recent advancements in therapeutic and diagnostic techniques for malignant gliomas, the median survival for patients with Grade III is less than five years, and for those diagnosed with Grade IV, it stands at a mere 15 months [5]. Table 1 presents various glioma grades categorized by their malignancy and level of aggressiveness. Neuroimaging data, particularly Magnetic Resonance Imaging (MRI) sequences such as T1C, T1W, T2W, and FLAIR (Fluid-Attenuated Inversion Recovery), offer precious insights into the size, shape, location, and metabolic activity of brain tumors [6]. These data serve as a crucial foundation for clinicians to assess the tumor's condition both before and after therapeutic interventions. The wealth of information contained in these images can be harnessed to distinguish between various brain tissues, facilitating the discrimination between tumor and normal [7–9].

Efficient management of gliomas necessitates two fundamental steps: the precise segmentation of the tumor to locate and characterize its various components and the accurate classification of the tumor to determine its grade. However, the conventional approach to these tasks involves manual intervention by physicians, which is not only laborious and time-consuming but also susceptible to inter-observer variability among specialists, thus potentially impeding the efficacy of treatment [10,11].

Table 1. Glioma grades and their characteristics.

Grades	Description
I	Slow growing tumor, Rarely spread to nearby tissues, Change in the structure of the cells is minimal, Relatively benign, Example: pilocytic astrocytoma.
II	Changes in the appearance of the tumor cells start to become evident, May spread into nearby tissues, Example: astrocytoma, oligodendroglioma and ependymoma.
III	The cells divide at a relatively high speed, Tumor cells infiltrate the neighbouring structures, High rate of hypercellularity, Example: anaplastic oligodendroglioma, anaplastic astrocytoma, and anaplastic ependymoma.
IV	Tumor cells grows abnormally fast, Very High rate of hypercellularity, Necrosis or cell death begins to start in the tumor, Example: glioblastoma.

Considering these challenges, the quest for automated diagnosis systems has gained momentum, aiming to equip clinicians with timely and precise morphological information about different tumor regions. This information is pivotal for facilitating prompt and accurate tumor diagnosis and treatment [11]. Recent decades have witnessed significant strides in medical image analysis, with machine learning (ML) emerging as a promising avenue. Traditional ML approaches, while effective, often entail the prerequisite of prior knowledge and manual feature extraction, which can be time-consuming [12]. In contrast, deep learning (DL), a more recent subfield of ML, has exhibited notable advantages in addressing the limitations of traditional ML based models. DL models can automatically extract intricate high-level features and seamlessly integrate feature extraction with classification/segmentation, streamlining the overall process [13,14]. Among the various DL approaches, Convolutional Neural Network (CNN) architectures have demonstrated superior performance, especially in the detection and analysis of neurological diseases [15]. To substantiate the viability of CNNs, they autonomously generate robust discriminative features through a hierarchical learning methodology. In the initial layers, feature maps extract fundamental low-level characteristics, while in subsequent layers, they capture more sophisticated, domain-specific attributes. The feature maps in the early layers encode basic structural elements such as edges, shapes, and textures, while the higher layers amalgamate these lower-level feature maps to construct abstract representations that encompass both local and global information. As a result, DL transforms manual feature extraction into a self-learning process. CNNs have been in existence for many years, but their popularity surged when Krizhevsky et al. [16] pioneered the use of DL with AlexNet. Simonyan and Zisserman [17] later introduced a similarly deep CNN, VGG Net, excelling in localization and classification tasks. The success of DL, particularly CNNs, can be attributed to advancements in computational technologies, such as powerful GPUs, and the evolution of learning algorithms. Some of the DL-based research efforts in glioma grading are discussed below.

Hao et al. [18] introduced a fully automated brain tumor detection and segmentation approach based on U-Net deep convolution networks, achieving efficient and robust segmentation results compared to manual ground truth delineation. Khawaldeh et al. [19] proposed the use of the AlexNet DL algorithm for identifying and grading abnormal brain MRIs; however, this method exhibited limitations in handling small datasets. Anaraki et al. [20] introduced gaussian assumption to streamline the selection of deep neural network architectures, eliminating the need for trial and error. They also employed an ensemble algorithm to reduce prediction errors, achieving an impressive 90.9% accuracy in classifying gliomas into three grades. Mzoughi et al. [21] leveraged volumetric T1-Gado MRI sequences to develop an automatic deep multi-scale 3D CNN model for glioma classification, achieving an overall accuracy of 96.49%.Zhuge et al. [22] utilized a modified U-Net model for segmentation and a 3D volumetric CNNs (3DConvNet) classification model to grade gliomas, attaining an accuracy of 97.1%.Gutta et al. [23] constructed a DCNN model for glioma classification and demonstrated its superiority over traditional ML models with an accuracy of 87%.Lu et al. [24] employed the ResNet model for glioma classification and incorporated pyramid dilated convolution to enhance performance; however, this method was limited to 2D MRI interpretation and required manual labeling of the training set. In a study by Naser et al. [25], a multi-task DL-based method was proposed, utilizing the U-Net architecture for segmentation and VGG-16 for classification. The reported dice score and tumor detection accuracy were 0.84 and 0.92, respectively. Decuyper et al. [26] trained a pipeline consisting of U-Net for segmentation and ResNet for classification, achieving an accuracy rate of 90% and a sensitivity rate of approximately 93.48%. Furthermore, Tandel et al. [27] developed

four therapeutically relevant datasets and employed five DL-based models (AlexNet, VGG-16, ResNet18, GoogleNet, and ResNet50) along with five ML-based models. They introduced the MajVot method to maximize classification performance and reported an improvement in average accuracy. In their subsequent work [28], they worked with five pre-trained CNNs, achieving a maximum accuracy of 99.06% through a majority voting technique. Nassar et al. [29] also used the concept of majority voting to the prediction outputs of five different CNN models (GoogleNet, AlexNet, SqueezeNet, ShuffleNet, and NasNet-Mobile) to get an accurate classification of brain tumors based on the T1c MRI dataset, which achieved an accuracy of 96.08%, 95.16%, 96.67%, 97.17% and 97.5% respectively.

From the brief literature review, it could be concluded that TL and ensemble learning emerge as the two predominant research-driven and application-oriented subfields in the realm of glioma classification and grading methods using DL. TL [30] leverages pre-trained neural network models, fine-tuning them to adapt to the specific characteristics of glioma data, thus capitalizing on the knowledge gained from other domains. Ensemble learning [31], on the other hand, encompasses a range of techniques that combine the predictions of multiple models to improve the overall accuracy and robustness of the classification and grading processes. These two subfields represent the forefront of research efforts in the quest for more accurate and clinically relevant solutions in the field of glioma analysis. Apart from this, the major drawbacks in most of the reviewed approaches for glioma classification and grading are summarized as follows:

- DL requires large, well-annotated datasets, which are often lacking in glioma research.
- Ensuring models perform well on diverse patient data is an ongoing challenge.
- Fine-tuning complex models demands substantial computational resources and expertise.
- Lack of standardized pre-processing affects data quality.
- Limited research has compared models with and without segmentation to evaluate the impact, and no studies provide clear statistical evidence for directly incorporating segmentation results into classification models.

The motivation for this research stems from the pressing need for more accurate, automated, and efficient methods in glioma diagnosis and grading. The complexity of gliomas, with their varied shapes, sizes, and locations within the brain, demands advanced image analysis techniques for accurate delineation. While advanced medical imaging techniques like MRI scans have enhanced our ability to visualize and diagnose brain tumors, manual analysis remains time-consuming and susceptible to human error. DL and image processing offer the potential to automate this process, potentially improving diagnostic accuracy and treatment planning reliability. In recent years several studies have explored various techniques, achieving promising results in tumor segmentation, classification, and even survival prediction. Although previous research has explored both segmentation and classification individually, fewer studies have focused on integrating them for a more comprehensive approach. Our novel contribution addresses this gap by integrating customized segmentation and classification architectures. Specifically, we have tailored the U-Net model for segmentation and the VGG-16 model for classification to better suit our research objectives. Our research leverages the BraTS2018 dataset, a widely recognized benchmark in the field of neuroimaging [32-34], to ensure the reliability and relevance of our findings. The methodology begins with preprocessing steps, including data splitting and application of gamma correction for enhanced image detail, and

normalization to standardize pixel values. Rotation augmentation is implemented to improve the model's generalization ability. Segmentation is performed using U-Net, featuring a tailored encoder-decoder, hybrid loss function and Leaky ReLU activation for improved gradient stability. For classification, we leverage fine-tuned VGG-16 model, incorporating strategic layer freezing for optimal performance. Both the segmentation and classification models undergo systematically tuned training, ensuring robust and accurate analysis throughout the study. While the novelty of our approach lies in the integration of these modified segmentation and classification architectures, this unique combination not only enables precise tumor localization but also provides a means to categorize gliomas into low-grade and high-grade groups, a critical factor in treatment planning. Leveraging this combined approach, our research aims to substantially contribute to ongoing efforts to improve glioma diagnosis and, consequently, enhance treatment outcomes by harnessing the capabilities of DL in medical imaging.

The paper is structured as follows: Section 2 introduces the proposed methodology, Section 3 showcases experimental results and analysis, Section 4 is dedicated to discussion and limitations, and finally, Section 5 concludes the research and provides future directions.

2. Materials and methods

2.1. Dataset

The proposed scheme is evaluated on BRaTS 2018 dataset obtained from Multimodal Brain Tumor Segmentation Challenge 2018. This dataset comprises 285 cases, including 210 High-Grade Gliomas (HGGs) and 75 Low-Grade Gliomas (LGGs). The dataset has been split into training, validation, and test subsets, and within the validation subset, there are 66 glioma tumors of various grades. The training set was further divided into 80% for training and 20% for testing, resulting in a total of 228 training images. The images are provided in NIfTI (Neuroimaging Informatics Technology Initiative) format, covering four modalities: T1W, T1C, T2W, and FLAIR. All the images within this dataset share a uniform volume dimension of 240×240×155, and they have been subject to careful manual annotation conducted by expert neuro-radiologists. This annotation aimed to delineate four distinct intra-tumoral regions, which include the necrotic core, non-enhancing, edema, and enhancing tumor areas. The dataset encompasses diverse glioma types with varying shapes, sizes, and locations within the brain. Each MRI sequence captures unique brain features using different scales, unlike standard images confined to a 0-255 gray value range. This variability stems from heterogeneous origin of the dataset, with scans acquired from various MRI scanners across different institutions. To address this inconsistency and ensure efficient training and inference, we normalize the voxel intensities using Equation 3. The schematic representation depicting the procedural framework employed in our study is illustrated in Figure 1.

2.2. Pre-processing

In the data preprocessing phase, the BraTS2018 dataset was prepared to ensure its suitability for training and evaluating the DL models. All scans were saved in neuroimaging format (i.e. nii.gz), so the first step is to convert nii.gz to 3D NumPy array. The use of gamma correction [35] was applied to address variations in image illumination and enhance the visibility of subtle structures within the MR

images. Mathematically, this correction can be represented as follows:

$$I_{corrected} = I_{orignal}^{\gamma} \tag{1}$$

where, γ is the correction factor.

Gamma correction was applied to enhance MRI modalities, except for FLAIR images. Gamma values of 2.3, 2.5, and 3 were chosen for T1W, T1C, and T2W modalities, respectively, to improve segmentation performance. This modality-specific gamma correction tailors contrast enhancement to each MRI type thereby optimizing the visibility of different tissue types and pathological features unique to each modality.

Additionally, data augmentation techniques, such as rotation, were employed to increase the diversity of the training data and improve the model's generalization ability [36]. Rotation augmentation helps the model become invariant to different orientations of gliomas within the images. This rotation operation can be expressed mathematically as:

$$I_{rotated} = rotate(I_{orignal,}\theta) \tag{2}$$

where, θ represent the rotation angle.

The value of θ ranging from 0 to 30 degrees are chosen randomly along one of the three dimensions of the 3D pictures to simulate variations in glioma orientation within the brain, ensuring that the model can handle tumors at different angles and positions. This range is chosen to introduce variability in the dataset without drastically altering the original image characteristics. Rotations within this range can simulate different patient orientations during MRI scans, making the model more robust to such variations in real-world scenarios. However, larger rotations might distort the anatomical structures in the images, leading to unrealistic scenarios and potentially misleading the model.

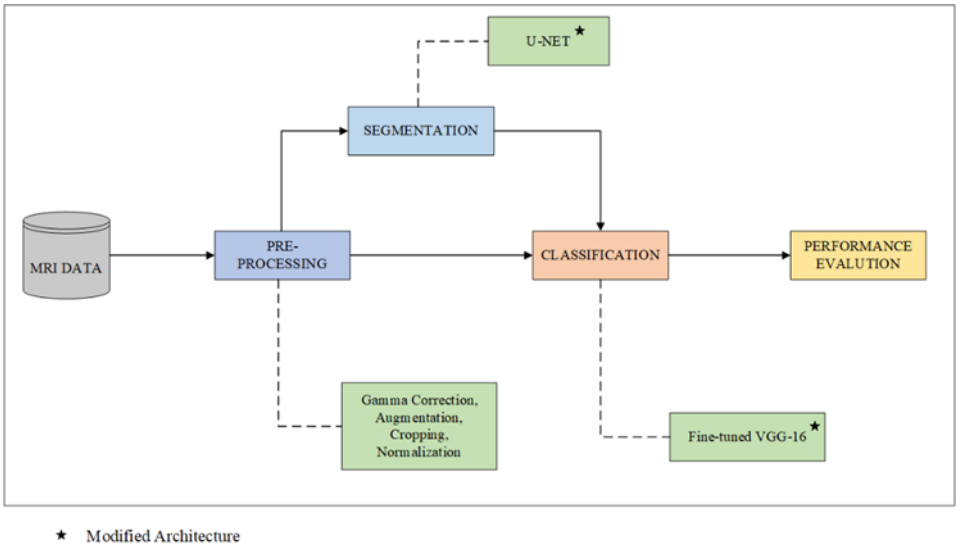

Figure 1. A flowchart of the methodology used in this study.

Furthermore, to ensure consistency in model input sizes and reduce computational complexity, the MRI images were cropped to a uniform size of 190×190×155 pixels. This size reduction was based on considerations of memory constraints and computational efficiency while still preserving relevant

anatomical information. Finally, data normalization was performed on each sequence of MRI images using the following equation:

$$I_{normalized} = \frac{I_{orignal} - \mu}{\sigma} \tag{3}$$

where, μ is the mean intensity value within the image, and σ is the standard deviation of the intensities within the image slices. Each MRI sequence is individually normalized using its own mean and standard deviation, instead of using dataset-wide values. This approach aims to improve generalizability while addressing the diverse intensity ranges encountered in our dataset, potentially leading to better model performance compared to standard normalization process. This normalization ensures that the input data are cantered and scaled appropriately for the DL models [37].

2.3. Segmentation

In this study, U-Net [38] is employed for glioma segmentation because of its exceptional architecture, featuring contracting and expansive pathways, which efficiently capture intricate anatomical structures and tumor boundaries in MR imaging data. Figure 2 illustrates the proposed model. Our network comprises five convolutional blocks, incorporated within both the encoder and decoder paths. These convolutional layers employ a 3x3 kernel size, facilitating the extraction of intricate spatial features while maintaining computational efficiency. A stride of 1 is consistently applied in both horizontal and vertical directions, ensuring meticulous convolutional operations across the input. Furthermore, a 2x2 maxpooling size is employed to down sample feature maps while retaining essential information. The activation function chosen is Leaky ReLU, for its capacity to mitigate the vanishing gradient problem [39]. For the final layer, the network adopts a softmax activation function, essential for pixel-wise classification in multi-class segmentation. Incorporating a dropout rate of 0.2 bolsters the network's robustness against overfitting while maintaining model expressiveness. The hybrid loss function employed in this study is defined by the following equation:

$$\text{Loss} = \alpha \times (\text{Categorical Cross Entropy}) + \beta \times (1 - \text{J\_tumor}) \tag{4}$$

Here, the weights α and β were set to 0.3 and 0.6, respectively, through a rigorous grid search process to find the optimal balance for our dataset. The α coefficient scales the contribution of the categorical cross entropy component, which is a standard choice for multi-class classification tasks [40]. However, it may not fully capture the desired segmentation quality, especially for imbalanced classes. To address this, we combine categorical cross entropy with jaccard index. Jaccard index measures the overlap between predicted and ground truth tumor regions, providing a good understanding of segmentation accuracy. The β coefficient is used to adjust the importance of the Jaccard similarity-based term, (1 − J_tumor), which is designed to encourage the model to focus on accurate segmentation of the tumor region. This loss function is a critical element of the network's training process, aiding in achieving the desired balance between classification accuracy and precise tumor region delineation. In terms of training, the network undergoes a learning rate of 0.01 and is trained for 8 epochs, the optimal settings established through iterative experimentation. For parameter optimization, the study employs the stochastic gradient descent (SGD) algorithm with a momentum of

0.99. The proposed model differs from the original U-Net by including a novel hybrid loss function, adopting Leaky ReLU activation to improve gradient stability, and implementing dropout regularization.

2.4. Classification

VGG-16 [17] is an established CNN architecture comprising a total of 16 layers organized into five convolutional blocks, with Leaky ReLU activation functions applied in each block. Following each block, max-pooling layers are applied, and the architecture is concluded with three fully connected layers, as illustrated in Figure 3. In pre-trained CNNs, the lower layers capture basic, general features, while the upper layers specialize in more intricate features. Consequently, we typically freeze the parameters of the earlier layers to maintain their focus on low-level features. In our current study, only the last three layers were kept trainable, primarily for classification purposes. For optimization, we utilized the SGD algorithm and employed categorical cross-entropy as the loss function [41]. Furthermore, we set specific hyperparameters, including a learning rate of 0.001, a batch size of 16, and ran training for 8 epochs The model's construction was executed using Keras, with TensorFlow serving as the backend framework. The novelty of our architecture, based on VGG-16, lies in its adaptation for glioma classification: transfer learning from a general domain to medical imaging, a customized output layer, strategic layer freezing, tailored hyperparameters, and the use of dropout for regularization. These adaptations enhance its suitability for the specific medical image classification task.

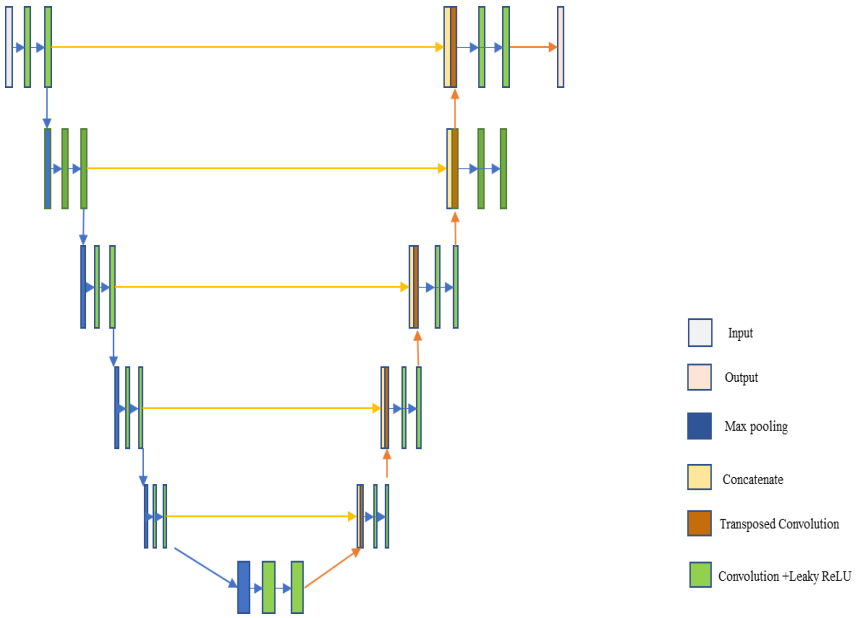

Figure 2. U-Net architecture.

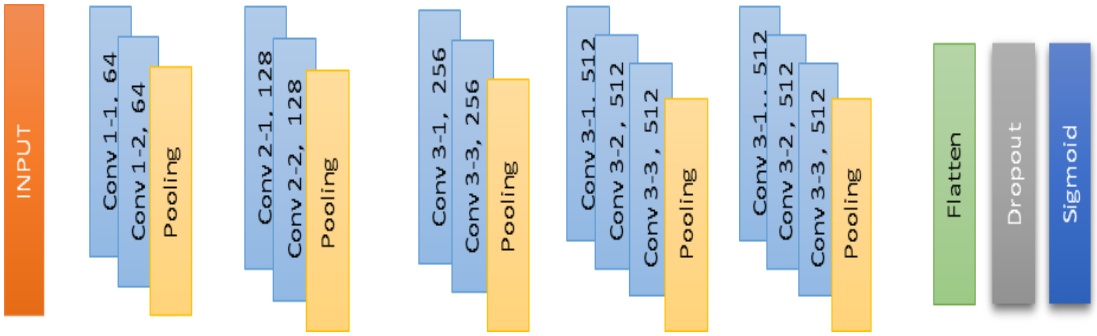

Figure 3. VGG-16 architecture.

3. Results

In this section, we present the results of glioma segmentation and classification using U-Net and VGG-16 models, followed by a comparative analysis with state-of-the-art methods. The proposed model, implemented using Python 3.7, TensorFlow 2.0, and Keras 2.3.1 frameworks, was evaluated on the BraTS 2018 dataset. Experiments were conducted on an Nvidia GeForce RTX 2080 Ti GPU with 11GB RAM. The initial preprocessing involved converting NIfTI images to 3D NumPy arrays and applying gamma correction, rotation augmentation, cropping, and normalization to enhance model robustness. For segmentation, we utilized a U-Net architecture featuring five convolutional blocks within both the encoder and decoder paths. Leaky ReLU activation, a hybrid loss function, and dropout regularization were incorporated to ensure accurate delineation of tumor regions. Classification leveraged a modified VGG-16 architecture with strategic layer freezing, tailored hyperparameters, and dropout. The final layers of the fine-tuned CNN models were adapted to accommodate the two tumor classes (LGG and HGG). Model optimization included a comprehensive grid search, optimizing key parameters like learning rate and dropout rate. Empirical observations revealed an inversely proportional relationship between learning rate/batch size and performance/training time. Consequently, smaller learning rates and batch sizes were chosen to improve performance. Model evaluation was conducted on the validation set using metrics: categorical cross entropy loss, jaccard index, and accuracy. Early stopping based on validation loss prevented overfitting, and robust 5-fold cross-validation ensured generalizability by continuously monitoring metrics within each fold.

3.1. Performance Evaluation Metrics

This study aims to determine the class of glioma tumors using MR images, which can determine whether a patient had LGG or HGG. Depending on the result discovered, output can be either positive or negative. The dice score [42] serves as a widely utilized validation metric for medical image segmentation, facilitating comparisons between automatic segmentation outcomes and ground truth, while the jaccard index offers another valuable measure for assessing the overlap and accuracy of segmentation results. Additionally, it assesses the reproducibility of segmentation. Accuracy, a key efficiency metric in the classification process, is employed when equal importance is assigned to both positive and negative classes. Recall measures the proportion of correctly predicted positive instances, while specificity identifies the percentage of accurately recognized true negatives [43]. Table 2 presents the metrics used to evaluate the model's effectiveness.

Table 2. Performance metrics and functionalities [42,43].

Metrics	Formula	Functionality
Accuracy	$\frac{T_p + T_n}{T_p + F_p + F_n + T_n}$	Proportion of correct model classifications
Specificity	$\frac{T_n}{T_n + F_p}$	Proportion of correctly identified negative instances
Recall	$\frac{T_p}{T_p + F_n}$	Proportion of correctly identified positive instances
Dice Score	$\frac{2\lvert T_p \cap T_a \rvert}{T_p + T_a}$	Measures overlap between predictions and ground truth
Jaccard Index	$\frac{\lvert T_p \cap T_a \rvert}{\lvert T_p \cup T_a \rvert}$	Measures similarity between predictions and ground truth

*T_p=True Positive, T_n= True Negative, F_p=False Positive, F_n=False Negative, T_a =Ground Truth

3.2. Glioma Segmentation with U-Net

Our utilization of the U-Net model for glioma segmentation yields compelling results, underscoring its efficacy in precisely delineating glioma regions within MR images. Table 3 summarizes glioma segmentation results using the U-Net model, showcasing high accuracy. The Dice Score values for whole tumor (WT), tumor core (TC) and enhanced tumor (ET) are 0.96, 0.92, and 0.89, respectively. The jaccard index values are 0.92, 0.85, and 0.80, and Recall values are 0.89, 0.94, and 0.87, indicating robust segmentation performance across different glioma regions. These results exhibit a substantial alignment with the ground truth.

Table 3. Glioma segmentation results with U-Net.

Metrics	WT	TC	ET
Dice Score	0.96	0.92	0.89
Jaccard Index	0.92	0.85	0.80
Recall	0.89	0.94	0.87

3.3. Glioma Classification with VGG-16

We further evaluate the performance of our model by classifying gliomas into LGGs and HGGs categories using the VGG-16 model. Classification results are presented in Table 4. These results offer valuable insights into the performance of our grading model on the BraTS 2018 dataset. The model

achieved an overall accuracy of 97.89%, indicating its ability to correctly classify glioma grades. All metrics exceeding 0.95 for both categories underscore the model's effectiveness in distinguishing between both grades. Figure 4(a) illustrates our model's ability to distinguish between LGG and HGG through a Receiver Operating Characteristic (ROC) curve. A higher curve and greater area under it indicate better classification accuracy. The comparison of the model's predictions against the actual ground truth labels for the BraTS 2018 dataset is illustrated in Figure 4(b).

Table 4. Glioma classification results with VGG-16 on BraTS2018 dataset.

Metrics	LGG	HGG
Accuracy (%)	97.89	97.89
Specificity (%)	97.44	98.24
Recall (%)	98.24	96.77

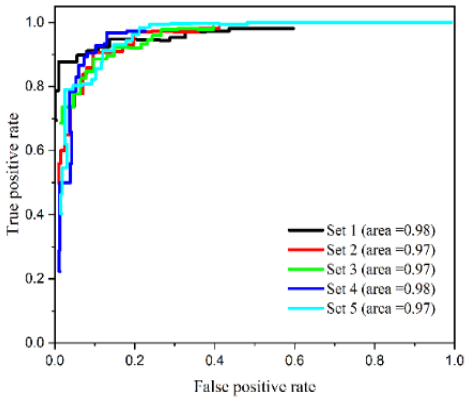

(a)

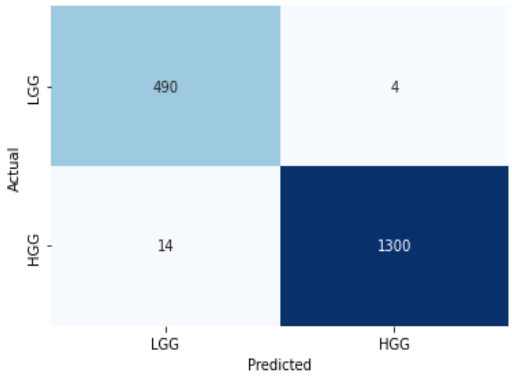

(b)

Figure 4. (a) ROC curve for the grading model with 5-fold cross validation. (b) Confusion matrix of BraTS 2018 based classification.

3.4. Comparison with State-of-the-Art

Table 5 presents a comprehensive comparative study of glioma segmentation methods, referencing various approaches and evaluating their performance. It investigates diverse DL based architectures and MRI modalities., Our model demonstrates superior performance compared to established methods, achieving remarkable dice scores of 0.96, 0.92, and 0.89 for WT, TC, and ET, respectively. Figure 5(a) complements Table 5 by visually representing the dice scores, enabling an at-a-glance comparison of the segmentation approaches. Figure 5(b) presents a visual comparison of the segmentation result and ground truth from a validation set sample image.

Table 5. Comparative study with state-of-the-art methods for glioma segmentation.

References	**Dataset**	**Sample Size**	**MRI Modalities**	**Architecture**	**Validation**	**Performance (Dice Score)**		
						WT	**TC**	**ET**
[44]	BraTS 2018	LGG:75 HGG:210	T1W, T2W, T1Wc, FLAIR	Deep Res-Unet	5-fold cross	0.95	0.93	0.90
[45]	BraTS 2018	LGG:75 HGG:210	T1W, T2W, T1Wc, FLAIR	Attention U-Net	5-fold cross	0.89	0.82	0.81
[46]	BraTS 2020	LGG:76 HGG:293	FLAIR	nnUNet	-	0.89	0.85	0.82
[47]	BraTS 2018	LGG:75 HGG:210	T1W, T2W, T1Wc, FLAIR	7 layers CNN	Random split sample	0.88	0.84	0.71
[48]	BraTS 2020	LGG:76 HGG:293	T1W, T2W, T1Wc, FLAIR	MAU-Net	5-fold cross	0.9185	0.8746	0.8350
[49]	BraTS 2018	LGG:75 HGG:210	T1W, T2W, T1Wc, FLAIR	BU-Net	-	0.901	0.837	0.788
[50]	BraTS 2019	LGG:76 HGG:259	T1W, T2W, T1Wc, FLAIR	RAAGR2-Net	-	0.896	0.821	0.776
Ours	BraTS 2018	LGG:75 HGG:210	T1W, T2W, T1Wc, FLAIR	Modified U-Net	5-fold cross	0.96	0.92	0.89

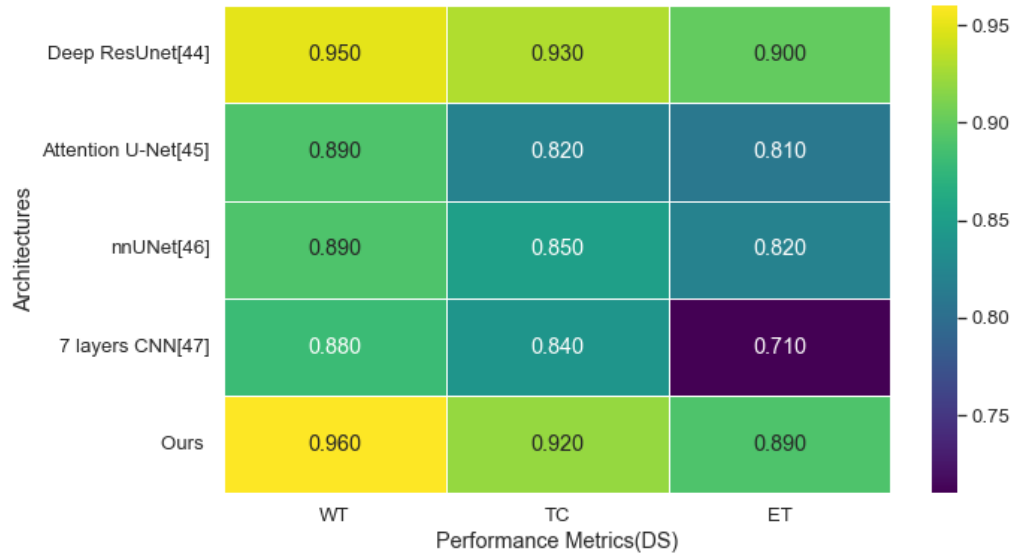

(a)

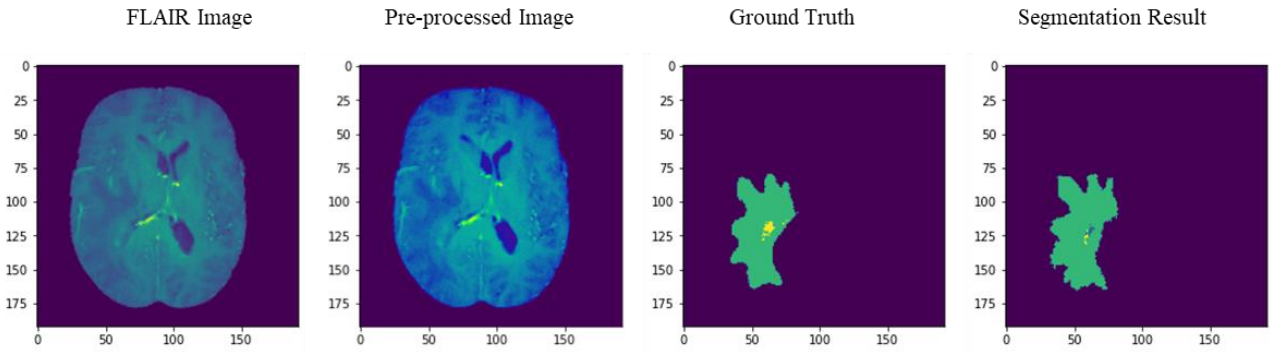

(b)

Figure 5. (a) Quantitative comparison of glioma segmentation methods, (b) Segmentation result for a sample image from validation set of BraTS 2018.

Table 6 provides a comprehensive comparative analysis of various glioma classification methods, shedding light on their performance across different datasets, MRI modalities, architectures, and validation techniques. Our proposed model achieves competitive accuracy in a 5-fold cross-validation on the BraTS 2018 dataset. To provide a visual representation of these accuracy comparisons among the models mentioned in the table, Figure 6 visually summarizes their performance. Table 7 provides a detailed comparison of different approaches, shedding light on their efficacy in improving the precision and accuracy of glioma grading by integrating DL based segmentation before grading. It highlights the potential benefits of integrating segmentation and classification, exemplified in the table, as they lead to enhanced precision and accuracy in grading which is crucial for guiding clinical decisions and improving patient care.

Table 6. Comparative study for glioma classification.

References	Dataset	Class	Sample Size	MRI Modalities	Architecture	Validation	Performance (%)		
							Accuracy	Recall	Specificity
[19]	TCIA	3	LGG:41 HGG:67 HEALTHY:22	FLAIR	12layers ConvNet	Random split sample	91.16	92.25	91.79
[51]	BraTS 2017	2	LGG:75 HGG:210	T1C	SE-ResNeXt-MLT	-	97.45	94.93	98.35
[52]	Tangdu Hospital of Fourth Militrary medical University	2	LGG:52 HGG: 61	T1C	Fine-tuned GoogLeNet	5-fold cross	96.8	-	-
[53]	BratTS 2020BratTS 2020	2	LGG :76 HGG: 293	T1W T2W T1Wc FLAIR	DenseNet121	Monte Carlo	97	97	97
[54]	BraTS 2019	2	LGG:75 HGG:210	T1W T2W T1Wc FLAIR T1-GD	7 stacked pretrained CNN	10-fold	98.06	98.06	98.67
[55]	BraTS 2019	2	LGG:76 HGG:259	T1W T2W T1Wc FLAIR	EfficientNetB0	Sample split in training and validation	98.87	-	-
[15]	Local Dataset	2	LGG:50 HGG: 54	T2W, FLAIR	Custom CNN	5-fold cross	97.1	98.0	96.3
Ours	BraTS 2018	2	LGG:75 HGG:210	T1W, T2W, T1Wc, FLAIR	Modified Pre-trained VGG-16	5-fold cross	97.89	97.50	97.84

Table 7. Comparative study for glioma grading integrating segmentation and classification.

References	**Dataset**	**Sample Size**	**MRI Modalities**	**Segmentation**	**Classification**	**Segmentation Performance**			**Classification Performance**
						Dice Score			Accuracy (%)
						WT	TC	ET	
[56]	BraTS 2019	LGG:259 HGG: 76	T1W, T2W, T1Wc, FLAIR	U-Net	VGG-16	0.91	0.72	0.82	97.44
[57]	TCIA	LGG:159 GBM:163	T2W	Cluster CNN	Fusion of ResNet/18/50/101/152	0.93			95.87
[22]	BraTS 2018BraTS 2018BraTS 2018	LGG:75 HGG:210LGG:75 HGG:210	T1W, T2W, T1Wc, FLAIR	3D U-Net	3DConvNet	-			97.1
[58]	BraTS 2020	LGG:76 HGG:293	T1W, T2W, T1Wc, FLAIR	ResNet-50	VGG-16	0.84			95
[59]	TCIA and BraTS 2015	-	T2W	U-Net and Handcrafted Features Extraction	VGG-16	-			96
Ours	BraTS 2018	LGG:75 HGG:210	T1W, T2W, T1Wc, FLAIR	Modified U-net	Modified Pre-trained VGG-16	0.96	0.92	0.89	97.89

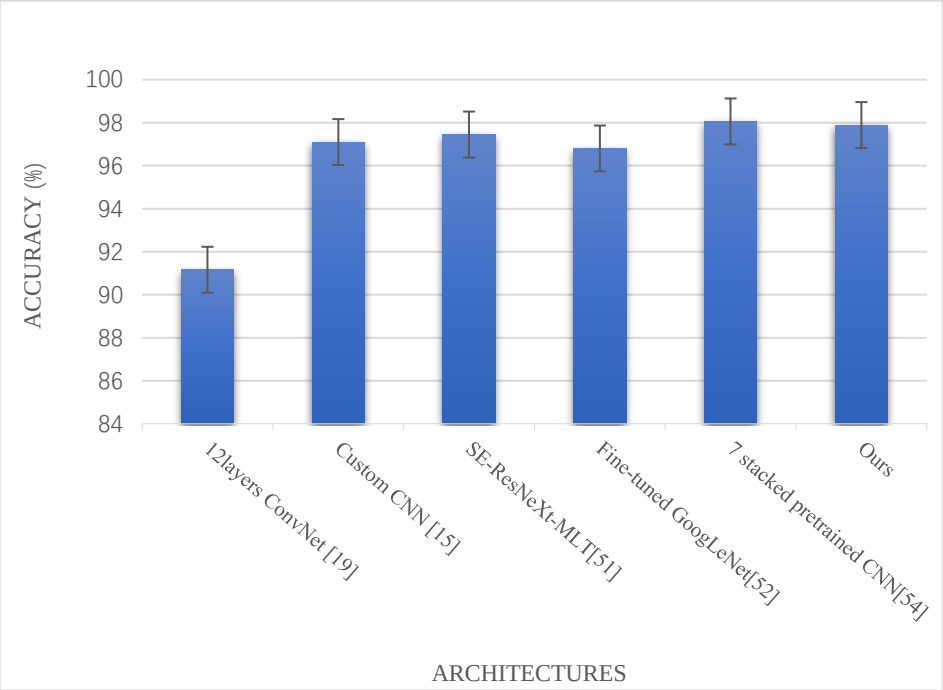

Figure 6. Comparison of our classification method with existing techniques on different datasets.

4. Discussion

In the existing body of literature, the interplay between segmentation and classification in the context of glioma analysis has been largely unexplored. Most studies have treated these as separate processes, focusing either on the segmentation of gliomas or on their classification into LGGs and HGGs. However, our approach addresses this gap by integrating segmentation and classification into a single, cohesive workflow. In this study, we explore the effectiveness of DCNNs using the tailored U-Net architecture for segmentation and the VGG-16 model for classification. Our primary aim is to simultaneously tackle glioma segmentation and classify gliomas into LGG and HGG categories using MRI data. To establish consistency and reliability in data pre-processing, we introduce a standardized methodology to ensures that our experiments are underpinned by a consistent pre-processing pipeline, ultimately enhancing data quality, and facilitating reproducibility. We strategically selected U-Net for segmentation and VGG-16 for classification, leveraging their complementary strengths. U-Net excels in capturing intricate anatomical structures and precise tumor boundaries, making it well-suited for detailed segmentation. Its unique architecture, incorporating skip connections, ensures the preservation of fine details crucial for accurate localization. The efficiency of U-Net in handling limited data and its end-to-end learning approach simplify the segmentation workflow. On the other hand, VGG-16, with its pre-trained layers, offers powerful feature extraction capabilities, enhancing computational efficiency through TL. It focuses on global patterns and class discrimination, making it ideal for classifying tumors into different subtypes based on overall characteristics. By combining U-Net's segmentation precision with VGG-16's feature extraction and classification abilities, we create a complementary workflow for comprehensive glioma analysis. This synergistic approach effectively addresses both the intricate details of tumor segmentation and the accurate

classification of glioma grades.

Our U-Net-based glioma segmentation demonstrates exceptional precision, as indicated by dice score values of 0.96, 0.92, and 0.89 for WT, TC, and ET, as detailed in Table 3. These results underscore the accuracy and reliability of our model in delineating glioma regions within MRIs. The robust jaccard index further validates the accuracy of our model's spatial predictions compared to ground truth. A distinguishing aspect of our research lies in the integration of these customized segmentation and classification architectures. Our fine-tuned VGG-16 classification model achieves an overall accuracy of 97.89%, complemented by high specificity and recall values exceeding 0.95 for both LGGs and HGGs, as presented in Table 4. These results demonstrate proficiency of our model in differentiating between these clinically significant categories.

To further emphasize the novelty and significance of our work, Table 5 provides a comprehensive comparative investigation into glioma segmentation methodologies, assessing a range of approaches, and evaluating the performance of the proposed model against state-of-the-art methods. Notably, most of these methods leverage U-Net as their foundation. This demonstrates the impact of U-Net, as its versatility has led to numerous modifications and extensions for diverse medical image segmentation tasks. Mahasin et al. [60] achieved 95% accuracy in head MRI tumor detection with both U-Net and UBNet, demonstrating its continued relevance. Similar successes span other modalities: Sateesh et al. [61] utilized super-resolution and federated TL for lung segmentation, while Ryu et al. [62] proposed SegR-Net for retinal vessel segmentation. Further, Tiwari et al. [63] and Ashwini et al. [64] leveraged modifications like inception modules and improved training strategies. Beyond U-Net, alternative methodologies have demonstrated notable accuracy. For instance, Ranjbarzadeh et al. [65] introduced a segmentation framework that integrates feature selection via the improved chimp optimization algorithm alongside hyperparameter optimization. In another study Ranjbarzadeh et al. [66] proposed a cascaded CNN model for mammogram classification. This model used 11 encoded images derived from the original mammogram via a GLCM-based encoding algorithm, allowing extraction of important features for breast and tumor tissue boundary detection. Additionally, Kasgari et al. [67] achieved notable performance by leveraging zernike moments and LDNP encoding, surpassing several conventional CNN approaches. Many more similar studies highlight the great impact of DL in the medical field [68]. Notably, while many of these studies achieved promising brain tumor segmentation results on BraTS, none addressed the crucial aspect of treatment response assessment through combined segmentation and classification, which remains our key contribution. Table 6 delivers an in-depth comparative analysis of glioma classification strategies, highlighting their performance across a diverse array of DL-based architectural frameworks. To facilitate benchmarking, we have compiled results from several relevant studies. Our proposed model achieved 97.89% accuracy, exceeding most reported results [51–53]. While Hamdaoui et al. [54] and Khazaee et al. [55] showed slightly higher accuracy, their studies focused solely on classification for treatment response assessment. Table 7 presents a comparative study for glioma grading that integrates both segmentation and classification. This table emphasizes our innovative approach and its performance, showcasing our method's superiority with other state-of-the-art techniques. Most significantly, this approach delves into the underexplored area of the impact of segmentation on classification, effectively bridging a notable gap in the existing literature. Our research contributes empirical evidence regarding the influence of segmentation on classification, adding depth to the understanding of glioma diagnosis.

Despite these achievements, it is crucial to acknowledge the limitations inherent in this study, particularly our reliance on data from a single institution. Future research endeavors should consider

the inclusion of data from multiple institutions to enable more extensive clinical trials and fortify the generalizability of our findings. Additionally, it is important to recognize that model performance may exhibit variations when applied to larger and more diverse datasets. Further refinement of the model architectures and hyperparameter tuning may lead to overall performance improvement, and these avenues represent potential future research directions.

While CNNs have dominated medical image segmentation, transformers are emerging as powerful alternatives. Many recent works have leverage transformers for improved accuracy and efficiency in medical image segmentation. Zhu et al. [69] propose a swin transformer-based method for brain tumor segmentation, combining it with CNNs for edge detection and feature fusion. Li et al. [70] introduce X-Net, a novel architecture combining CNNs and transformers for enhanced local and global feature extraction. Xianyu et al. [71] present a cloud-based segmentation method using transformers and CNNs, overcoming limitations in local computing power. Yang et al. [72] propose a hybrid network integrating CNNs and transformers with a multi-dimensional statistical feature extraction module for improved texture feature extraction. Building upon these works, future studies could investigate novel architectures that leverage the strengths of transformers, potentially combining them with CNNs or other techniques for even more accurate and efficient segmentation. Such advancements hold immense potential for further refining glioma diagnosis.

5. Conclusion

In this research, we have presented a comprehensive approach for glioma segmentation and classification using DL models, specifically U-Net for segmentation and VGG-16 for classification. Our primary goal is to identify the most optimum channel for glioma grading and assess the significance of segmentation in classification models. Glioma segmentation with U-Net achieved high DS values of 0.96, 0.92 and 0.89 for WT, TC, and ET respectively, on the test dataset, demonstrating the model's ability to accurately outline tumor regions in MRI images. Furthermore, the glioma classification using the fine-tuned VGG-16 model resulted in an impressive accuracy of 97.89%, with consistently high specificity and recall values above 0.95 for both grades. These results highlight the model's ability to distinguish between different glioma grades. The synergy between U-Net and VGG-16 adds a layer of depth to our methodology, resulting in improved accuracy in glioma grading.

This study underscores the potential utility of DL-based glioma segmentation and classification in the field of medical imaging. By demonstrating the effectiveness of this integrated approach, our study provides empirical evidence supporting the hypothesis that accurate segmentation can indeed enhance the performance of subsequent classification. This finding not only validates our methodology but also opens new avenues for future research in this domain. We believe that our work will inspire further investigations into the synergistic effects of segmentation and classification, ultimately leading to more accurate and reliable glioma diagnosis. Future research should focus on integrating additional clinical data and developing real-time diagnostic tools for practical use in clinical settings. Additionally, broader clinical trials involving data from multiple institutions would enhance the generalizability of our findings.

Use of AI tools declaration

The authors declare they have not used Artificial Intelligence (AI) tools in the creation of this article.

Acknowledgments

We would like to thank Department of Computer Science and Engineering, National Institute of Technology Agartala, Tripura, India for their support related to infrastructure. No funds gathered by any of the sources.

Conflict of interest

The authors declare there is no conflict of interest.

References

1. M. L. Goodenberger, R. B. Jenkins, Genetics of adult glioma, *Cancer Genet.*, **205** (2012), 613–621. https://doi.org/10.1016/j.cancergen.2012.10.009
2. D. N. Louis, A. Perry, G. Reifenberger, A. Deimling, D. Figarella-Branger, W. K. Cavenee, et al., The 2016 World Health Organization Classification of Tumors of the Central Nervous System: A summary, *Acta Neuropathol.*, **131** (2016),803–820. https://doi.org/10.1007/s00401-016-1545-1
3. D. N. Louis, A. Perry, P. Wesseling, D. J. Brat, I. A. Cree, D. Figarella-Branger, et al., The 2021 WHO Classification of Tumors of the Central Nervous System: A summary, *Neuro-Oncol.*, **23** (2021),1231–1251.https://doi.org/10.1093/neuonc/noab106
4. J. S. Barnholtz-Sloan, Q. T. Ostrom, D. Cote, Epidemiology of brain tumors, *Neurol. Clin*., **36** (2018), 395–419. https://doi.org/10.1016/j.ncl.2018.04.001
5. M. Decuyper, R.V. Holen, Fully automatic binary glioma grading based on Pre-therapy MRI using 3D Convolutional Neural Networks, preprint, arXiv:1908.01506
6. A. Patra, A. Janu, A. Sahu, MR Imaging in neurocritical care*, Indian J. Crit. Care Med.*, **23** (2019), 104–114. https://doi.org/10.5005/jp-journals-10071-23186
7. Ö. Polat, C. Güngen, Classification of brain tumors from MR images using deep transfer learning, *J. Supercomput.*, **77** (2021), 7236–7252.https://doi.org/10.1007/s11227-020-03572-9
8. S. Gore, T. Chougule, J. Jagtap, J. Saini, M. Ingalhalikar, et al., A review of radiomics and deep predictive modeling in glioma characterization, *Acad. Radiol.*, **28** (2021), 1599–1621. https://doi.org/10.1016/j.acra.2020.06.016
9. H. Jiang, Z. Diao, Y. Yao, DL techniques for tumor segmentation: A review, *J. Supercomput.,* **78** (2022), 1807–1851. https://doi.org/10.1007/s11227-021-03901-6
10. S. Waite, J.Scott, B. Gale, T. Fuchs, S. Kolla, D. Reede, Interpretive error in radiology*, Am. J. Roentgenol.*, **208** (2017), 739–749. https://doi.org/10.2214/ajr.16.16963
11. R. Ranjbarzadeh, A. B. Kasgari, S. J. Ghoushchi, S. Anari, M. Naseri, M. Bendechache, Brain tumor segmentation based on DL and an attention mechanism using MRI multi-modalities brain images, *Sci. Rep*., **11** (2021), 10930. https://doi.org/10.1038/s41598-021-90428-8
12. M.-A. Schulz, B. T. Thomas Yeo, J. T. Vogelstein, J. Mourao-Miranada, J. N. Kather, K. Kording, Different scaling of linear models and deep learning in UKBiobank brain images versus machine-learning datasets, *Nat. Commun*., **11** (2020). https://doi.org/10.1038/s41467-020-18037-z
13. K. Yasaka, H. Akai, A. Kunimatsu, S. Kiryu, O. Abe, Deep learning with convolutional neural network in radiology, *Jpn. J. Radiol*., **36** (2018), 257–272. https://doi.org/10.1007/s11604-018-0726-3

14. S. Fathi, M. Ahmadi, A. Dehnad, Early diagnosis of Alzheimer, *Comput. Biol. Med.*, **146** (2022), 105634. https://doi.org/10.1016/j.compbiomed.2022.105634
15. H. Özcan, B. G. Emiroglu, H. Sabuncuoğlu, S. Özdoğan, A. Soyer, T. Saygı, A comparative study for glioma classification using deep convolutional neural networks, *Math. Biosci. Eng*., **18** (2021),1550–1572. https://doi.org/10.3934/mbe.2021080
16. A. Krizhevsky, I. Sutskever, G. E. Hinton, ImageNet classification with deep convolutional neural networks, *Commun. ACM*, **60** (2017), 84–90. https://doi.org/10.1145/3065386
17. K. Simonyan, A. Zisserman, Very deep convolutional networks for large-scale image recognition, (2014), preprint, arXiv:1409.1556.
18. H. Dong, G. Yang, F. Liu, Y. Mo, Y. Guo, Automatic brain tumor detection and segmentation using U-Net based fully Convolutional Networks, preprint, arXiv:1705.03820
19. S. Khawaldeh, U. Pervaiz, A. Rafiq, R. S. Alkhwaldeh, Noninvasive grading of glioma tumor using magnetic resonance imaging with Convolutional Neural Networks, *Appl. Sci*., **8** (2017), 27. https://doi.org/10.3390/app8010027
20. A. K. Anaraki, M. Ayati, F. Kazemi, Magnetic resonance imaging-based brain tumor grades classification and grading via convolutional neural networks and genetic algorithms, *Biocybern. Biomed. Eng*., **39** (2019), 63–74. https://doi.org/10.1016/j.bbe.2018.10.004
21. H. Mzoughi, I. Njeh, A. Wali, M. B. Slima, A. B. Hamida, C. Mhiri, et al., Deep multi-scale 3D Convolutional Neural Network (CNN) for MRI Gliomas brain tumor classification, *J. Digit. Imaging*, **33** (2020), 903–915. https://doi.org/10.1007/s10278-020-00347-9
22. Y. Zhuge, H. Ning, P. Mathen, J. Y. Cheng, A. V. Krauze, K. Camphausen, et al., Automated glioma grading on conventional MRI images using deep convolutional neural networks, *Med. Phys*., **47** (2020), 3044–3053. https://doi.org/10.1002/mp.14168
23. S. Gutta, J. Acharya, M. S. Shiroishi, D. Hwang, K. S. Nayak, Improved Glioma grading using Deep Convolutional Neural Networks, *AJNR Am. J. Neuroradiol*., **42** (2020), 233–239. https://doi.org/10.3174/ajnr.a6882
24. Z. Lu, Y. Bai, Y. Chen, C. Su, S. Lu, T. Zhan, et al., The classification of gliomas based on a Pyramid dilated convolution resnet model, *Pattern Recognit. Lett.*, **133** (2020), 173–179.https://doi.org/10.1016/j.patrec.2020.03.007
25. M. A. Naser, M. J. Deen, Brain tumor segmentation and grading of lower-grade glioma using deep learning in MRI images, *Comput. Biol. Med.*, **121** (2020), 103758. https://doi.org/10.1016/j.compbiomed.2020.103758
26. M. Decuyper, S. Bonte, K. Deblaere, R. Van Holen, Automated MRI based pipeline for segmentation and prediction of grade, IDH mutation and 1p19q co-deletion in glioma, *Comput. Med. Imaging Graph.*, **88** (2021), 101831. https://doi.org/10.1016/j.compmedimag.2020.101831
27. G. S. Tandel, A. Tiwari, O. Kakde, Performance optimisation of deep learning models using majority voting algorithm for brain tumour classification, *Comput. Biol. Med.*, **135** (2021), 104564. https://doi.org/10.1016/j.compbiomed.2021.104564
28. G. S. Tandel, A. Tiwari, O. G. Kakde, Performance enhancement of MRI based brain tumor classification using suitable segmentation method and deep learning-based ensemble algorithm, *Biomed. Signal Process. Control.*, **78** (2022). https://doi.org/10.1016/j.bspc.2022.104018
29. S. E. Nassar, I. Yasser, H. M. Amer, M. A. Mohamed, A robust MRI-based brain tumor classification via a hybrid deep learning technique, *J. Supercomput.*, **80** (2023). https://doi.org/10.1007/s11227-023-05549-w

30. T.-Y. Hsiao, Y.-C. Chang, C.-T. Chiu, Filter-based deep-compression with global average pooling for Convolutional Networks, in *IEEE International Workshop on Signal Processing Systems (SiPS)*, (2018). https://doi.org/10.1109/sips.2018.8598453
31. T. G. Dietterich, Ensemble methods in machine learning, in multiple classifier systems, MCS 2000. *Lecture Notes Computer Sci.*, **1857** (2020). https://doi.org/10.1007/3-540-45014-9_1
32. B. Menze, A. Jakab, S. Bauer, J. Kalpathy-Cramer, K. Farahani, J. Kirby, et al., The Multimodal Brain Tumor Image Segmentation Benchmark (BRATS), *IEEE Trans. Med. Imaging*, **34** (2015), 1993–2024. https://doi.org/10.1109/TMI.2014.2377694
33. S. Bakas, M. Reyes, A. Jakab, S. Bauer, M. Rempfler, A. Crimi, et al., Identifying the best machine learning algorithms for brain tumor segmentation, progression assessment, and overall survival prediction in the BRATS challenge, (2018), preprint, arXiv:1811.02629.
34. S. Bakas, H. Akbari, A. Sotiras, M. Bilello, M. Rozycki, J. S. Kirby, et al., Advancing the Cancer genome atlas glioma MRI collections with expert segmentation labels and radiomic features, *Sci. Data*, **4** (2017). https://doi.org/10.1038/sdata.2017.117
35. A. Man, S. Anand, Method of multi-region tumour segmentation in brain MRI images using grid-based segmentation and weighted bee swarm optimisation*, IET Image Process.*, **14** (2020), 2901–2910. https://doi.org/10.1049/iet-ipr.2019.1234
36. K. Maharana, S. Mondal B. Nemade, A review: Data pre-processing and data augmentation techniques, *Glob. Transit.*, **3** (2022), 91–99. https://doi.org/10.1016/j.gltp.2022.04.020
37. H. Moradmand, S. M. R. Aghamiri, R. Ghaderi, Impact of image preprocessing methods on reproducibility of radiomic features in multimodal magnetic resonance imaging in glioblastoma, *J. Appl. Clin. Med. Phys.*, **21** (2019),179–190. https://doi.org/10.1002/acm2.12795
38. O. Ronneberger, Invited Talk: U-Net Convolutional Networks for Biomedical Image Segmentation, in *Bildverarbeitung für die Medizin 2017, Informatik aktuell*, (2017), 3. https://doi.org/10.1007/978-3-662-54345-0_3
39. S. Das, M. K. Swain, G. K. Nayak, S. Saxena, S. C. Satpathy, Effect of learning parameters on the performance of U-Net Model in segmentation of Brain tumor, *Multimed. Tools Appl.*, **81** (2021), 34717–34735. https://doi.org/10.1007/s11042-021-11273-5
40. A. Rusiecki, Trimmed categorical cross-entropy for deep learning with label noise, *Electron. Lett*., **55** (2019), 319–320. https://doi.org/10.1049/el.2018.7980
41. H. Seo, M. Bassenne, L. Xing, Closing the gap between deep neural network modeling and biomedical decision-making metrics in segmentation via adaptive loss functions, *IEEE Trans. Med. Imaging*, **40** (2021) ,585–593. https://doi.org/10.1109/tmi.2020.3031913
42. A. Taha, A. Hanbury, Metrics for evaluating 3D medical image segmentation: Analysis, selection, and tool, *BMC Med. Imag*., **15** (2015). https://doi.org/10.1186/s12880-015-0068-x
43. A. Tharwat, Classification assessment methods, *Appl. Comput. Inform*., **17** (2020), 168–192. https://doi.org/10.1016/j.aci.2018.08.003
44. C. Huan, M. Wan, Automated segmentation of brain tumor based on improved U-Net with residual units, *Multimed. Tools Appl*., **81** (2022), 12543–12566. https://doi.org/10.1007/s11042-022-12335-y
45. M. Noori, A. Bahri, K. Mohammadi, Attention-guided version of 2D UNet for automatic brain tumor segmentation, in *9th International Conference on Computer and Knowledge Engineering (ICCKE),* (2019). https://doi.org/10.1109/iccke48569.2019.8964956

46. F. Isensee, P. F. Jager, P. M. Full, P. Vollmuth, K. H. Maier-Hein, NnU-Net for brain tumor segmentation, in *Brainlesion: Glioma, Multiple Sclerosis, Stroke and Traumatic Brain Injuries, BrainLes 2020, Lecture Notes in Computer Science*, **12659**. https://doi.org/10.1007/978-3-030-72087-2_11
47. W. Ayadi, W. Elhamzi, M. Atri, A deep conventional neural network model for glioma tumor segmentation, *Int. J. Imaging Syst.*, **33** (2023),1593–1605. https://doi.org/10.1002/ima.22892
48. Y. Zhang, Y. Han, J. Zhang, MAU-Net: Mixed attention U-Net for MRI brain tumor segmentation, *Math Biosci. Eng.,* **20** (2023),20510–20527. https://10.3934/mbe.2023907
49. M. U. Rehman, S. Cho, J. H. Kim, K. T. Chong, BU-Net: Brain tumor segmentation using modified U-Net architecture, *Electronics*, **9** (2020), 2203. https://doi.org/10.3390/electronics9122203
50. M. U. Rehman, J. Ryu, I. F. Nizami, K. T. Chong, RAAGR2-Net: A brain tumor segmentation network using parallel processing of multiple spatial frames, *Comput. Biol. Med*., **152** (2023), 106426. https://doi.org/10.1016/j.compbiomed.2022.106426
51. J. Linqi, N. Chunyu, L. Jingyang, Glioma classification framework based on SE-ResNeXt network and its optimization, *IET Image Process*., **16** (2021), 596–605. https://doi.org/10.1049/ipr2.12374
52. Y. Yang, L-F. Yan, X. Zhang, Y. Han, H-Y. Nan, Y-C. Hu, et al., Glioma grading on Conventional MR Images: A deep learning study with transfer learning, *Front. Neurosci*., **12** (2018), 804. https://doi.org/10.3389/fnins.2018.00804
53. S. V. Rubio, M. T. Garcia-Ordas, O. García-Olalla Olivera, H. Alaiz-Moretón, M. González-Alonso, J. A. Benítez-Andrades, Survival and grade of the glioma prediction using transfer learning, *PeerJ Comput. Sci*., **9** (2023). https://doi.org/10.7717/peerj-cs.1723
54. H. E. Hamdaoui, A. Benfares, S. Boujraf, N. E. H. Chaoui, B. Alami, M. Maaroufi, et al., High precision brain tumor classification model based on deep transfer learning and stacking concepts, *Indones. J. Electr.*, **24** (2021), 167–177. https://doi.org/10.11591/ijeecs.v24.i1.pp167-177
55. Z. Khazaee, M. Langarizadeh, and M. E. Shiri Ahmadabadi, Developing an artificial intelligence model for tumor grading and classification, based on MRI sequences of human brain gliomas, *Int. J. Cancer Manag.*, **15** (2022). https://doi.org/10.5812/ijcm.120638
56. K. Dang, T. Vo, L. Ngo, H. Ha, A deep learning framework integrating MRI image preprocessing methods for brain tumor segmentation and classification, *IBRO Neurosci. Rep.*, **13** (2022), 523–532. https://doi.org/10.1016/j.ibneur.2022.10.014
57. P. C. Tripathi, S. Bag, A computer-aided grading of glioma tumor using deep residual networks fusion, *Comput. Methods Programs Biomed*., **215** (2022), 106597. https://doi.org/10.1016/j.cmpb.2021.106597
58. A. B. Slama, H. Sahli, Y. Amri, H. Trabelsi, Res-Net-VGG19: Improved tumor segmentation using MR images based on Res-Net architecture and efficient VGG gliomas grading, *Appl. Eng. Sci*., **16** (2023), 100153. https://doi.org/10.1016/j.apples.2023.100153
59. J. Sivakumar, S. R. Kannan, K. S. Manic, Automated classification of brain tumors into LGG/HGG using concatenated deep and handcrafted features, in *Frontiers of Artificial Intelligence in Medical Imaging*, (2022). https://doi.org/10.1088/978-0-7503-4012-0ch7
60. M. M. Mahasin, A. Naba, C. S. Widodo, Y. Yueniwati, Development of a modified UNet-based image segmentation architecture for brain tumor MRI segmentation, in *Proceedings of the International Conference of Medical and Life Science (ICoMELISA 2021)*, (2023), 37–43. https://doi.org/10.2991/978-94-6463-208-8_7

61. S. Ambesange, B. Annappa, S. G. Koolagudi, Simulating federated transfer learning for lung segmentation using modified UNet model, *Procedia Comput. Sci.*, **218** (2023), 1485–1496. https://doi.org/10.1016/j.procs.2023.01.127
62. J. Ryu, M. U. Rehman, I. F. Nizami, K. T. Chong, SegR-Net: A deep learning framework with multi-scale feature fusion for robust retinal vessel segmentation, *Comput. Biol. Med.*, **163** (2023), 107132. https://doi.org/10.1016/j.compbiomed.2023.107132
63. T. Tiwari, M. Saraswat, A new modified-unet deep learning model for semantic segmentation, *Multimed. Tools Appl.*, **82** (2023), 3605–3625. https://doi.org/10.1007/s11042-022-13230-2
64. A. K. Upadhyay, A. K. Bhandari, Semi-supervised modified-UNet for lung infection image segmentation, *IEEE Trans. Radiat. Plasma Med. Sci*., **7** (2023), 638–649. https://doi.org/10.1109/trpms.2023.3272209
65. R. Ranjbarzadeh, P. Zarbakhsh, A. Caputo, E. B. Tirkolaee, M. Bendechache, Brain tumor segmentation based on optimized convolutional neural network and improved chimp optimization algorithm, *Comput. Biol. Med.*, **168** (2024), 107723. https://doi.org/10.1016/j.compbiomed.2023.107723
66. R. Ranjbarzadeh, S. J. Ghoushchi, N. T. Sarshar, E. B. Tirkolaee, S. S. Ali, T. Kumar, et al., ME-CCNN: Multi-encoded images and a cascade convolutional neural network for breast tumor segmentation and recognition, *Artif. Intell. Rev.*, **56** (2023), 10099–10136. https://doi.org/10.1007/s10462-023-10426-2
67. A, B. Kasgari, R. Ranjbarzadeh, A. Caputo, S. B. Saadi, M. Bendechache, Brain tumor segmentation based on zernike moments, enhanced ant lion optimization, and convolutional neural network in MRI images, metaheuristics and optimization, in *Computer and Electrical Engineering, Lecture Notes in Electrical Engineering*, **1077** (2023). Springer, Cham. https://doi.org/10.1007/978-3-031-42685-8_10
68. S. Anari, N. S. Tataei, N. Mahjoori, S. Dorosti, A. Rezaie, Review of deep learning approaches for Thyroid Cancer Diagnosis, *Math. Probl. Eng*., (2022), 1–8. https://doi.org/10.1155/2022/5052435
69. Z. Zhu, X. He, G. Qui, Y. Li, B. Cong, Y. Liu, Brain tumor segmentation based on the fusion of deep semantics and edge information in multimodal MRI, *Inf. Fusion*, **91** (2023), 376–387. https://doi.org/10.1016/j.inffus.2022.10.022
70. Y. Li, Z. Wang, L. Yin, Z. Zhu, G. Qi, Y. Liu, X-Net: A dual encoding–decoding method in medical image segmentation, *Vis. Comput.*, **39** (2021), 2223–2233. https://doi.org/10.1007/s00371-021-02328-7
71. X. He, G. Qi, Z. Zhu, Y. Li, B. Cong, L. Bai, Medical image segmentation method based on multi-feature interaction and fusion over cloud computing, *Simul. Model Pract. Theory*, **126** (2023), 102769. https://doi.org/10.1016/j.simpat.2023.102769
72. Y. Xu, X. He, G. Xu, G. Qi, K. Yu, Li. Yin, et al., A medical image segmentation method based on multi-dimensional statistical features, *Front. Neurosci.*, **16** (2022). https://doi.org/10.3389/fnins.2022.1009581